Anisotropic Coupling in Hexagonal Arrays of Asymmetric Nickel Nano-Rings

Evgeny Sirotkin and Feodor Y. Ogrin

School of Physics, University of Exeter, Exeter, EX4 4QL U.K.

Here we report experimental studies of the orientational effects due to anisotropic coupling in hexagonal arrays of asymmetric Ni nano-rings. The remanent magnetization and coercive field were examined as a function of applied field angle in two samples with different orientations of asymmetry of the shape with respect to the principal axis of the lattice. It was found that the angular variation of coercive field follows a two-fold symmetry while the remanence exhibits a four-fold variation. The four-fold variation is more pronounced when the symmetry axis of the shape is in the same direction as the principal axis of the lattice. As seen from micromagnetic simulations the coupling arising from closely packed elements in a hexagonal array does not significantly affect the "vortex" state, but it does affect the remanent state of the system. Here we show that by changing the direction of the symmetry of the ring with respect to the lattice orientation one can manipulate the hysteretic dependence of the system.

Index Terms—**Anisotropic coupling, asymmetric nano-rings, etched nano-sphere lithography, hexagonal array.**

I. Introduction

ASYMMETRIC ferromagnetic nano-rings have recently attracted much interest as a system with deterministic direction of "vortex" circulation [1]–[5]. The attention is partly due to the current research attempts to find stable magnetic flux-closure state systems for magneto-electronic applications [6]. In such applications the control of the "vortex" chirality in patterned circular elements is essential for controlling the bistability of the magnetic state, so asymmetric ferromagnetic nano-rings, where chirality is guided by the asymmetry, are potentially very promising [2], [4]. The storage density is another factor which is important in any magneto-electronic application. The effective storage density is determined by both element size and element separation. The latter is the cause of strong coupling for close-packed designs. It has been shown [7], [8] that the coupling between rings affects the magnetization reversal and the remanent state. However the influence of orientational effects has not yet been considered.

In this work we report on the experimental results of the angular dependence of magnetic switching and coupling in large area hexagonal arrays of close-packed asymmetric Ni rings. The results are given for two samples in which the symmetry axis of the ring is parallel and at $\sim 30^\circ$ away from the principal axis of the hexagonal lattice [Fig. 2(c)–(e)]. The magnetic hysteresis loops were acquired for different angular orientations of the magnetic field applied in the plane of the lattice. We show that the angular variation of the coercivity (H_c) and remanence (M_r) have similar two-fold symmetry dictated by the asymmetry of the shape of the rings. However, the exact form of the dependence is different for the two samples. From the results of micromagnetic simulations we speculate that the anisotropies observed in the angular dependences of H_c and M_r are due to the interplay of the shape-anisotropy of the rings and the effect of anisotropic coupling which arises from the hexagonal lattice. In particular, from angular variation of M_r we can see two types of anisotropy (uniaxial and four-fold) when the symmetry axes of the rings and the lattice are aligned. Thus, we demonstrate that by changing the direction of the symmetry axis of the ring with respect to the orientation of the array one can modify the average hysteretic properties of the sample.

Manuscript received October 30, 2009; revised December 17, 2009; accepted December 31, 2009. Corresponding author: E. Sirotkin (e-mail: e.sirotkin@exeter.ac.uk).

Digital Object Identifier 10.1109/TMAG.2010.2040716

II. Fabrication

To investigate the anisotropic properties of the coupling, large-area highly ordered hexagonal arrays of close-packed asymmetric Ni rings have been fabricated by adapting techniques based on the combination of etched nanosphere lithography [9], [10], e-beam evaporation, and argon-ion milling. A close-packed monolayer of polystyrene spheres [9] has been used to create a nanoscale shadowing mask for angle-resolved evaporation of magnetic metal. After evaporation, exposed areas around spheres were milled out with argon-ion beam which was applied at 15° to the normal of the sample plane. The inclination of the beam is thus directly responsible for the asymmetry in the shape of the ring [11]. The milling plane was chosen to be parallel and at 30° to the principal axis of the array, which was identified from scanning electron microscopy (SEM) images. Rings have an outer/inner diameter of 650 nm/400 nm with asymmetry in width of 50 nm, center-to-center separation of 780 nm, edge-to-edge separation of 130 nm, and thickness of 20 nm. The arrays have a well-defined orientation of hexagonal array axes exhibiting long range ordering over areas of 5×5 mm^2. Fig. 1 shows an SEM image of a fragment from a typical array of rings which can be produced using the described technique.

III. Experiment

Magnetic properties have been investigated by longitudinal magneto-optical Kerr effect (MOKE). A HeNe laser was used as an s-polarized light source, and a magnetic field was applied in the plane of the sample. The sample was placed in the focal plane of converging lens, which was used to produce a spot size of approximately 500 μm. Since the periodicity in the array was preserved over an area of 25 mm^2, this spot size ensured that the area probed was well within an ordered region.

Magnetization loops have been measured over the entire range of 360° with 10° intervals. In Fig. 2 we show experimental hysteresis loops (cross-marked line) for fields applied

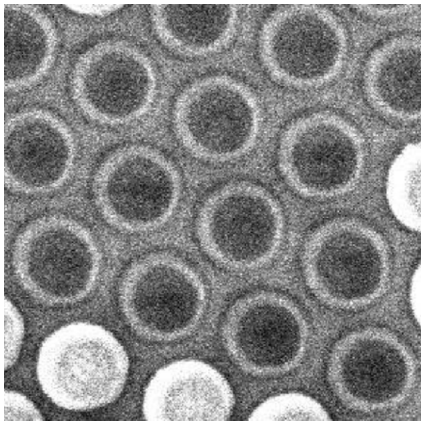

Fig. 1. SEM image of an example of the ring-structures produced by the described method after removal of the sphere-mask. The grayscale between rings corresponds to 3 nm of Cr which was sputtered for enhanced contrast. Remaining spheres, which were left in order to demonstrate the fabrication technique, are shown as white regions.

along two characteristic directions: a) perpendicular and b) parallel to the symmetry axis of the rings. Both shown cases are for the sample where the symmetry axis of the rings is parallel to the principal axis of the array (see insets). An arrow in the inset schematics indicates the direction of the applied field. Simulated loops (dashed lines) presented on the same plots have been extracted from the central element modelled within a seven element hexagonal cell. In the case of the perpendicular orientation of the field [Fig. 2(a)] the hysteresis loop exhibits a smooth reversal with slight narrowing, which indicates more favourable formation of a "vortex" configuration at lower field. The hysteresis loop for the parallel orientation has a significant widening in H_c which suggests a more stable remanent state, such as an "onion" configuration. At the same time, from the shape of the measured hysteresis loops and the fact that neighboring rings interact, we believe that the average magnetic response is formed from a combination of different micromagnetic configurations. This is qualitatively confirmed by micromagnetic simulations.

Exploring the change in the shape of the measured hysteresis loops as function of the orientation of the applied field we can plot the angular dependence of H_c and M_r (see Figs. 3 and 4, respectively). The change in H_c and M_r has been used as a measure of the configurational anisotropy of the array [10]. The direction along 0° for both angular scans corresponds to the direction of applied field along the symmetry axis of the rings. Having analysed the experimental scans of H_c and M_r we have derived the following conclusions.

1) Angular uniaxial anisotropy of the coercivity results from the shape anisotropy of asymmetric rings. A transition from an easy to a hard axis has been observed as the applied field was rotated 90° away from the symmetry axis of rings. Anisotropic coupling of the array does not affect significantly the coercivity (H_c) because all rings at that field are in the "vortex" state which is stray-field free.
2) Magnetic switching between different states (e.g., "onion"—"vortex") is the result of interplay between the shape anisotropy of the ring and the effect of anisotropic coupling in the array.

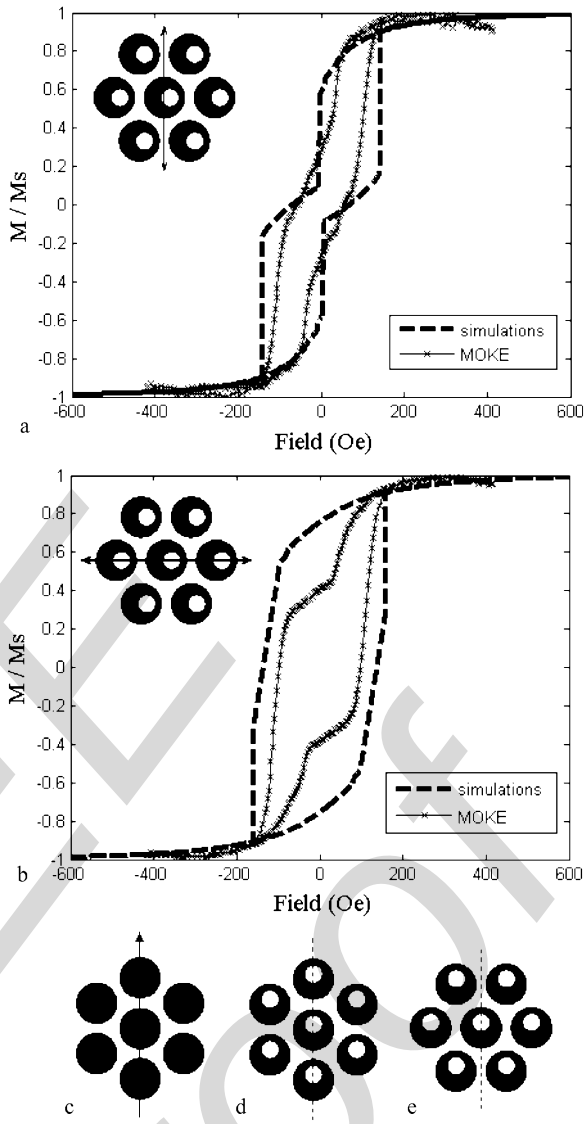

Fig. 2. Hysteresis loops obtained from hexagonal arrays of asymmetric rings where the symmetry axis of the ring is parallel to the principal axis of the array. In (a) the field is applied perpendicular to the symmetry axis of the rings while in (b) the field is applied along the symmetry axis of the rings. Cross-marked lines are loops measured using longitudinal MOKE. Bold-dashed lines are simulated loops extracted from the central element of seven rings (as shown in the inset). Insets show the directions of applied field along characteristic directions. Simulations were performed using the 3-D OOMMF solver using a mesh of $200 \times 221 \times 1$ cells with cell size of $10 \times 10 \times 20$ nm^3, and material parameters determined from experimental results. (c) Definition of the "principal" axis of a hexagonal array (shown with arrow), i.e., axis along the nearest neighbors (the sketch is shown for dots in order to simplify the graphical definition). (d) and (e) Configurations for asymmetric rings with symmetry axis (dotted line) parallel and 30° away from the principal axis respectively.

3) A change in the angular anisotropy can be seen from the angular variation of remanence (M_r) for two different structures. In the sample where the symmetry axis of the rings is at 30° (i.e., in between) to the principal axes of the lattice the angular dependence is almost uniaxial. For the configuration where the symmetry axis of the rings is parallel to one of the principal axes a four-fold symmetry structure can be observed.

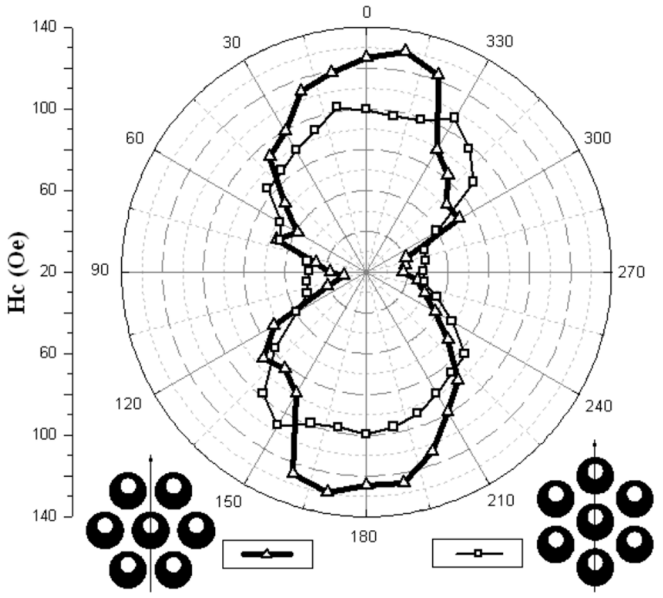

Fig. 3. Angular dependence of coercivity for both array configurations shown in the insets (experimental points extracted from hysteresis loops). The solid line connecting the experimental points serves as guide for the eye. Arrows in the insets show the orientation of the symmetry axis of the ring.

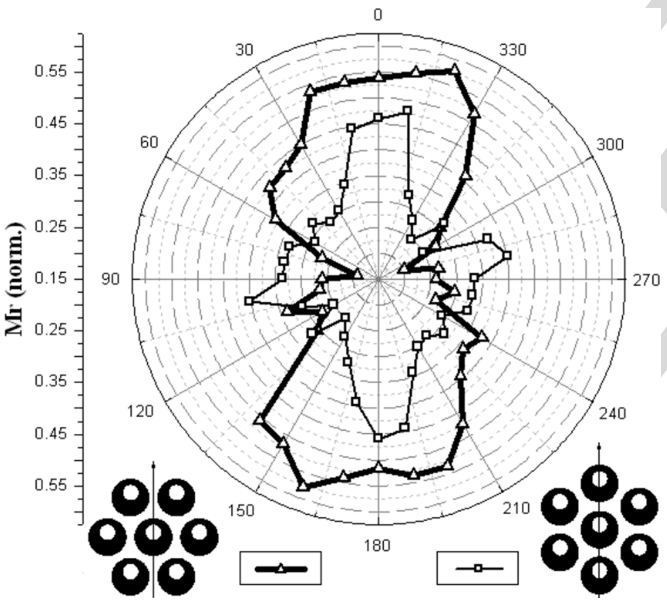

Fig. 4. Remanent magnetization (experimental points extracted from hysteresis loops) as function of angle of the applied field for both array configurations as shown in the insets. The solid line connecting the experimental points serves as guide for the eye.

In order to further understand the origin of the observed anisotropy, micromagnetic simulations were performed using the object oriented micromagnetic framework (OOMMF) [12].

A hexagonal array consisting of a single element surrounded by six nearest neighbors was constructed. Simulated hysteresis loops were extracted from the central element only. The cell-size of $10 \times 10 \times 20$ nm^3 was chosen to be reasonably small to account for exchange interactions (exchange length for $\mathrm{Ni} \sim 15$ nm). The edge roughness in simulated rings due to discrete mesh $(10 \times 10$ nm$^2)$ is similar, if not slightly larger, than in

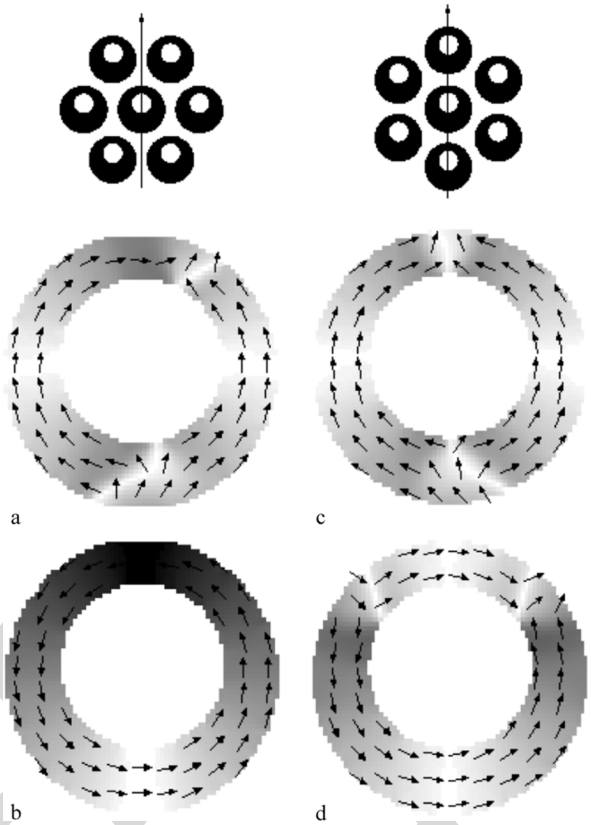

Fig. 5. Simulated micromagnetic maps of magnetization at remanence for the central element within a hexagonal seven-element unit cell. The left-hand panel shows the configuration in which the symmetry axis of the rings is at 30° to the principal axis of the array. In (a) the field is applied parallel to the symmetry axis, while in (b) the field is applied perpendicular to the symmetry axis. The right-hand panel shows the configuration where the two symmetry axes are aligned. In (c) the field is applied parallel and (d) perpendicular to the symmetry axis of the rings.

rings measured experimentally (∼5 nm). Geometric parameters, such as diameter and separation of rings, were taken from SEM images and the saturation magnetization $Ms = 280$ emu/cm^3 was measured using a vibrating sample magnetometer. Saturation magnetization of the magnetic material was found to be lower than the commonly quoted number of 485 emu/cm^3. We speculate that the reduction is probably due to the ion-milling process and partial oxidation of the material. From the micromagnetic simulation of an individual asymmetric Ni ring we find that when the applied field is parallel to the symmetry axis of the ring the remanent state has "onion" configuration. This state is preferable, since it is energetically favourable for the domain wall to be localized in the narrow arm of ring. When the external field is applied perpendicular to the symmetry axis, the remanent state is a "vortex" configuration. The situation is different for ring surrounded by neighbors due to the strong dipolar coupling from adjacent rings. When the field is applied along the symmetry axis of the rings the remanent state in both array configurations is "onion" [see Fig. 5(a) and (c)]. This explains the high remanence in this direction (see Fig. 4). However, when the field is applied perpendicular to the symmetry axis, the configurations for these two different cases become different. For the configuration with 30∘ misalignment (left-hand inset, Fig. 4) the central ring is in a "vortex" state [see Fig. 5(b)]

and thus exhibiting the lower remanence in hysteresis. In this case switching to "vortex" is additionally assisted by the dipolar interactions with neighboring rings. For the case with the parallel alignment of the axes (right-hand inset, Fig. 4), the central ring is found to have a higher remanent magnetization [see Fig. 5(d)] with two domain walls trapped in the narrow section of the ring. From simulations for this configuration we believe that the "onion" state is more stable here as a result of stray fields from wider sections of adjacent rings. Generally, in this configuration the alternative arrangement of wider and narrower sections of the adjacent rings increases the stray "magnetizing" fields in the narrow sections, while keeping the "demagnetizing" fields the same. This effectively creates an additional anisotropic direction for the whole pattern so that a four-fold symmetry in the remanence angular dependence is observed.

Comparing the experimental and simulated values of remanence for both array configurations for each characteristic field orientation (parallel and perpendicular to the symmetry axis of rings) we can see good qualitative agreement. For example, for the first array configuration (Fig. 4, left-hand inset) the experimental relation $M_r(\text{perp})/M_r(\text{paral}) = 0.33$, which corresponds to the simulated result of $M_r(\text{perp})/M_r(\text{paral}) = 0.14$. For the second array configuration (Fig. 4, right-hand inset) the experimental value $M_r(\text{perp})/M_r(\text{paral}) = 0.85$ corresponds to the simulated result of $M_r(\text{perp})/M_r(\text{paral}) = 0.78$. The actual values of the remanence and coercivity and also the shape of the simulated hysteresis loops are, however, quite different (as seen from Fig. 2). This can be understood in terms of limitations of the simulation model. Due to limiting computational power the simulations were carried out for seven rings. Given the symmetric arrangement within the hexagonal cell, the central ring is exposed to the external dipolar fields from all its six neighbors, so the stray field effect for this ring is correctly approximated (disregarding negligible dipolar effects from the next-nearest neighbors). However, each of the six "edge" rings have only three nearest neighbors. Therefore, the magnetic configurations of these rings may not be modelled correctly since the stray fields will be different to that of the measured array. This will affect the configuration of the field produced by each edge element. Nevertheless, we believe that the stray fields are only the second-order effect compared to the demagnetizing fields (shape anisotropy) of each element itself, so the seven-element hexagonal cell, as described here, is a good approximation of the dipolar effects in a whole lattice. It is interesting to note that in both configurations the "vortex" chirality of the central ring within the hexagonal cell is always found to be the same as that of the individual ring (i.e., the moment in the wider part of the ring is parallel to the initial direction of the applied field).

So, it is believed that anisotropic coupling does not affect the average chirality of "vortices" in the array, again supporting the above view that the shape anisotropy of the ring is the dominant factor in demagnetizing effects.

IV. Conclusion

The effects of anisotropic coupling in a hexagonal system of asymmetric rings have been studied. It was found that two types of coupling symmetry, uniaxial and four-fold, can be observed when the symmetry axis of the ring is displaced from the principal axis of the lattice. By modifying the angle between these two directions one can modify the values of the remanent magnetization and the coercivity in the hysteretic properties of the whole array. These effects may be potentially useful for magneto-electronic applications.

Acknowledgment

The authors gratefully acknowledge the financial support of the University of Exeter Research Fund in this work. The authors also would like to thank Prof. Rob Hicken for the valuable discussions on this work, Dr. Paul Keatley for advice on performing the magneto-optical measurements, and Mr. Dave Jarvis for technical support during sample preparation.

References

[1] P. Vavassori, R. Bovolenta, V. Metlushko, and B. Ilic, "Vortex rotation control in Permalloy disks with small circular voids," *J. Appl. Phys.*, vol. 99, p. 053902, 2006.

[2] E. Saitoh, M. Kawabata, K. Harii, H. Miyajima, and T. Yamaoka, "Manipulation of vortex circulation in decentered ferromagnetic nanorings," *J. Appl. Phys.*, vol. 95, no. 4, p. 1986, 2004.

[3] F. Giesen, J. Podbielski, B. Botters, and D. Grundler, "Vortex circulation control in large arrays of asymmetric magnetic rings," *Phys. Rev. B*, vol. 75, p. 184428, 2007.

[4] R. Nakatani *et al.*, "Magnetization chirality due to asymmetrical structure in Ni-Fe annular dots for high-density memory cells," *J. Appl. Phys.*, vol. 95, no. 11, p. 6714, 2004.

[5] S. Prosandeev, I. Ponomareva, I. Kornev, and L. Bellaiche, "Control of vortices by homogeneous fields in asymmetric ferroelectric and ferromagnetic rings," *Phys. Rev. Lett.*, vol. 100, p. 047201, 2008.

[6] C. A. F. Vaz *et al.*, "Ferromagnetic nanorings," *J. Phys.: Condens. Matter*, vol. 19, p. 255207, 2007.

[7] M. Kläui, C. A. F. Vaz, J. A. C. Bland, and L. J. Heyderman, "Domain wall coupling and collective switching in interacting mesoscopic ring magnet arrays," *Appl. Phys. Lett.*, vol. 86, p. 032504, 2005.

[8] J. Wang, A. O. Adeyeye, and N. Singh, "Magnetostatic interactions in mesoscopic Ni80Fe20 ring arrays," *Appl. Phys. Lett.*, vol. 87, p. 262508, 2005.

[9] S. M. Weekes, F. Y. Ogrin, W. A. Murray, and P. S. Keatley, "Macroscopic arrays of magnetic nanostructures from self-assembled nanosphere templates," *Langmuir*, vol. 23, p. 1057, 2007.

[10] S. M. Weekes, F. Y. Ogrin, and P. S. Keatley, "Configurational anisotropy in hexagonal arrays of submicron Co elements," *J. Appl. Phys.*, vol. 99, p. 08B102, 2006.

[11] F. Q. Zhu, G. W. Chern, O. Tchernyshyov, X. C. Zhu, J. G. Zhu, and C. L. Chien, "Magnetic bistability and controllable reversal of asymmetric ferromagnetic nanorings," *Phys. Rev. Lett.*, vol. 96, p. 027205, 2006.

[12] M. J. Donahue and D. G. Porter. [Online]. Available: http://math.nist.gov/oommf/